JOURNAL OF MATERIALS SCIENCE **39** (2004) 903–909

Preparation and characterization of copolymerized methylsilsesquioxane-benzylsilsesquioxane microparticles for electrophoretic sol-gel deposition

A. MATSUDA*, T. TANAKA, K. TADANAGA, T. MINAMI, M. TATSUMISAGO
Department of Applied Materials Science, Graduate School of Engineering, Osaka Prefecture University, Sakai, Osaka 599-8531, Japan
E-mail: matsuda@tutms.tut.ac.jp

Copolymerized methylsilsesquioxane-benzylsilsesquioxane, $(100 - x)\mathrm{MeSiO}_{3/2}\cdot x\mathrm{BnSiO}_{3/2}$ (mol%), microparticles of 0.3–0.4 μm in average diameter have been prepared by the sol-gel method and applied to the formation of thick films on indium tin oxide (ITO)-coated glass substrates by the electrophoretic deposition. The microparticles obtained were considered to be hybrid containing both methyl and benzyl groups from thermal analyses and structural investigations. The microparticles became fusible at $x \geqq 80$ by a heat treatment. Thick film, ca. 5 μm thick, consisting of electrophoretically deposited pure $\mathrm{BnO}_{3/2}$ microparticles became transparent upon thermal sintering of the particles during heat treatment at temperatures higher than 100°C. On the other hand, the increase in optical transmittance during the heat treatment of the films consisting of $20\mathrm{MeSiO}_{3/2}\cdot 80\mathrm{BnSiO}_{3/2}$ microparticles was as small as about 20% in visible range even after the heat treatment. The smaller increase in transmittance is probably due to the relatively high viscosity of the $20\mathrm{MeSiO}_{3/2}\cdot 80\mathrm{BnSiO}_{3/2}$ upon sintering in comparison with pure $\mathrm{BnO}_{3/2}$ for elimination of the voids in the films. © *2004 Kluwer Academic Publishers*

1. Introduction

The sol-gel method is an excellent procedure to prepare thin coating films on various substrates [1, 2]. However, the thickness of the coating films prepared by the conventional sol-gel method like dip- and spin-coating techniques is generally limited to be less than 1 μm due to cracking, although thicker films are required for several practical applications [3, 4]. Electrophoretic deposition is a useful way for the preparation of thick films on substrates with a complicated shape in much shorter time compared to the other coating techniques [5, 6]. We have proposed the "electrophoretic sol-gel deposition method", which is combined sol-gel method for particle preparation and electrophoretic deposition of the sol-gel derived particles, for the preparation of thick films of ca. 20 μm in thickness [7–9]. The films prepared by the electrophoretic sol-gel deposition are composed of spherical SiO_2 particles of sub-micrometers in diameter derived from tetraethoxysilane. These thick films are usually opaque because the scattering of light occurs at the interface between particles in the films.

Recently, we have developed a new technique to form transparent, inorganic-organic thick films on substrates by using organosilisesquioxanes in the $\mathrm{PhSiO}_{3/2}$-$\mathrm{BnSiO}_{3/2}$ system for the electrophoretic sol-gel deposition aiming at the application to micro-optic devices [10–12]. The process of the technique developed is as follows: (i) preparation of $\mathrm{PhSiO}_{3/2}$-$\mathrm{BnSiO}_{3/2}$ microparticles from organoalkoxysilanes by the sol-gel method, (ii) electrophoretic deposition of the particles in sol on the substrate used as an electrode, and (iii) improvement in transparency of the deposited film on the substrate due to the thermal sintering of the microparticles by a heat treatment. Patterned thick films with a convex shape for optical component can be fabricated on glass substrates with patterned indium tin oxide (ITO) coating when the microparticles dispersed in the sol are selectively deposited on the patterned area on which dc voltage is applied [12]. The most important process to obtain transparent, thick films by this process is the thermal sintering of the microparticles during a heat treatment, which causes the morphological change of the films from the aggregate of the organosilsesquioxane particles to the continuous layer. The thermal sintering properties can be controlled by changing hydrolysis and condensation conditions as well as by changing the chemical composition of the microparticles. For example, the onset temperature for

---

Present address: Department of Materials Science, Toyohashi University of Technology, 1-1 Hibarigaoka, Tempaku-cho, Toyohashi, Aichi 441-8580, Japan.

thermal sintering of the $PhSiO_{3/2}$-$BnSiO_{3/2}$ microparticles decreased from 150 to 50°C with an increase in $BnSiO_{3/2}$ content [13]. The onset temperature of $PhSiO_{3/2}$ microparticles can also be lowered from 270 to 110°C by decreasing the condensation time from 120 to 0.5 h under basic conditions [14]. The thermal sintering of the particles was a unique phenomenon observed in the $PhSiO_{3/2}$-$BnSiO_{3/2}$ system; the other silsesquioxane particles such as methyl-, ethyl-, vinyl- and allyl-silsesquioxanes do not become continuous layer through the thermal sintering.

In the present study, copolymerized methylsilsesquioxane-benzylsilsesquioxane ($MeSiO_{3/2}$-$BnSiO_{3/2}$) microparticles have been prepared by the sol-gel method using the corresponding organotrialkoxysilanes as the starting materials. $MeSiO_{3/2}$ shows low refractive index and no thermal sintering, whereas $BnSiO_{3/2}$ has high refractive index and low thermal sintering temperature. Therefore, the hybridization of $MeSiO_{3/2}$ with $BnSiO_{3/2}$ should provide the copolymerized microparticles with thermal sintering properties to form continuous films in the electrophoretic deposition and subsequent heat treatment, and should permit the control of the optical properties of the resultant films. The particle size, molecular weight, refractive index and thermal sintering behavior of the obtained $MeSiO_{3/2}$-$BnSiO_{3/2}$ microparticles have been examined aiming at the application to the sol-gel electrophoretic deposition. In addition, structural changes in the particles with hybridization of $MeSiO_{3/2}$ and $BnSiO_{3/2}$ components have been discussed.

2. Experimental procedures

2.1. Preparation of copolymerized $MeSiO_{3/2}$-$BnSiO_{3/2}$ microparticles

Fig. 1 shows the preparation procedures of copolymerized $(100 - x)MeSiO_{3/2}{\cdot}xBnSiO_{3/2}$ microparticles ($x = 0$, 20, 40, 60, 80 and 100 mol%) by the sol-gel method. The preparation conditions were determined on the basis of the conditions reported previously for the preparation of copolymerized $PhSiO_{3/2}$-$BnSiO_{3/2}$ microparticles [14]. Methyltriethoxysilane ($MeSi(OEt)_3$) and benzyltriethoxysilane ($BnSi(OEt)_3$) were used as the starting materials. Aqueous hydrochloric acid containing HCl of 0.03 mass% was added to the $MeSi(OEt)_3$ and $BnSi(OEt)_3$ individually for hydrolysis. These organosilanes are immiscible with hydrochloric acid, so that emulsions consisting of droplets of the organosilanes dispersed in hydrochloric acid were obtained under vigorous stirring. Before mixing, the $MeSi(OEt)_3$ emulsion was stirred at 25°C for 20 min and the $BnSi(OEt)_3$ emulsion for 18 h until they became homogeneous solutions. The homogeneous and clear solutions obtained were mixed and stirred at 25°C for 30 min. The mixed solution was then added to ammonia water containing NH_3 of 1 mass%. In a short time after mixing, the solution became a milky turbid sol due to the formation of $MeSiO_{3/2}$-$BnSiO_{3/2}$ microparticles, and the resultant sol was further stirred at 25°C for principally 8 h. The molar ratio of total organoalkoxysilanes/H_2O (in hydrochloric acid)/H_2O (in ammonia water) was fixed to be 1/20/180. The $MeSiO_{3/2}$-$BnSiO_{3/2}$ microparticles were collected by centrifugation and were dried under *vacuo* of about 1 Torr at room temperature for 3 h.

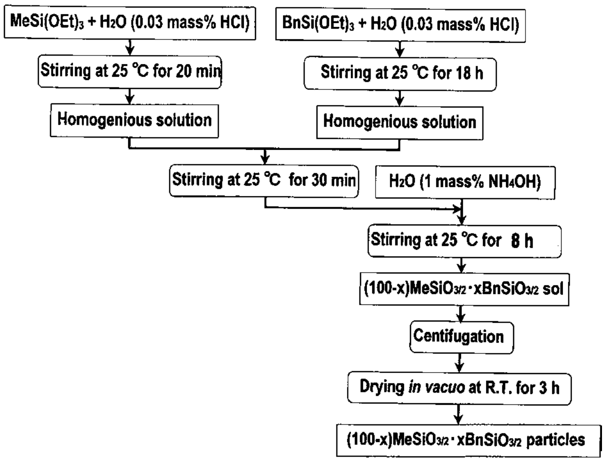

Figure 1 Preparation procedures of copolymerized $MeSiO_{3/2}$-$BnSiO_{3/2}$ microparticles by the sol-gel method.

2.2. Characterization of $MeSiO_{3/2}$-$BnSiO_{3/2}$ microparticles

Average size and distribution of $MeSiO_{3/2}$-$BnSiO_{3/2}$ microparticles were examined using a scanning electron microscope (SEM) (Jeol Model JSM-5300). Refractive index of the microparticles was evaluated using refractive index standard liquids (Cargille Laboratories, Series AAA, AA and A). The weight average molecular weights of the microparticles were measured using a gel permeation chromatography (GPC), which was composed of a pump (Shimadzu Model LC-10AD), a detector (Shimadzu RID-6A), and a column oven (Shimadzu CTO-10A), using tetrahydrofuran as the eluent at 40°C.

Thermal softening behaviors of the $MeSiO_{3/2}$-$BnSiO_{3/2}$ microparticles with respect to the sintering were observed on SEM. The $MeSiO_{3/2}$-$BnSiO_{3/2}$ microparticles obtained were stepwise heat-treated at temperatures up to 200°C for 30 min at 10°C intervals in ambient air. Thermal stability and burning of organic groups of $MeSiO_{3/2}$-$BnSiO_{3/2}$ microparticles were observed using thermogravimetry and differential thermal analysis (MAC Science, TG-DTA2000), and Fourier-transform infrared spectroscopy (Perkin Elmer, FT-IR1600). Glass transition temperature of the microparticles was obtained from differential scanning calorimetry (Perkin Elmer, DSC 7) at a heating rate of 10°C min^{-1}. Structural units of the microparticles were examined using a ^{29}Si cross polarization magic-angle spinning (CPMAS)-NMR (Varian, Model Unity Inova 300). The NMR spectra were measured at 59.59 MHz, 4.7 μs of 90° pulse length, 10 s of decay between pulses, and a spinning rate of 3000–4000 Hz. Tetramethylsilane was used as an external standard.

For the preparation of the thick films by the electrophoretic sol-gel deposition, ethanol was added to the resultant ammonia sols where the weight ratio of ammonia water:ethanol was 1:1. The ITO-coated glass plate was used as a substrate for the formation of thick film coatings and for measurement of optical transmittance. Stainless steel spiral (SUS304BA) was used as a counter electrode. A constant dc voltage was applied between the two electrodes, i.e., the ITO-coated glass plate and the spiral, by using a power supply. The dried films were heat-treated in air at temperatures between 50 and 400°C for 2 h. Optical transmission spectra of the substrates coated with the $MeSiO_{3/2}$-$BnSiO_{3/2}$ thick films on ITO-coated glass substrates were measured by an ultraviolet-visible-light spectrophotometer (JASCO, Model V-560).

3. Results and discussion

3.1. Physical properties and structure of microparticles

Fig. 2 shows SEM images of the $(100-x)MeSiO_{3/2}\cdot xBnSiO_{3/2}$ microparticles obtained. The average particle size and the standard deviation of the microparticles are shown in Table I. The average particle size is in the range from 0.3 to 0.4 μm and almost independent of the composition, whereas the standard deviation increases with an increase in x, i.e., $BnSiO_{3/2}$ content. In the pre-hydrolysis process of organosilanes in hydrochloric acid, $MeSi(OEt)_3$ and $BnSi(OEt)_3$ were respectively stirred for 20 min and 18 h at 25°C to obtain homogeneous and clear solutions, which is attributed to the lower hydrolysis rate of $BnSi(OEt)_3$ due to the steric effect of bulky benzyl group. Such a lower hydrolysis rate probably causes the wide distribution in nucleation and growth of microparticles, and results in the increase in standard deviation of the particle size [15].

TABLE I Average size and standard deviation of $(100-x)MeSiO_{3/2}\cdot xBnSiO_{3/2}$ microparticles

x (mol%)	0	20	40	60	80	100
Average size (μm)	0.37	0.32	0.36	0.35	0.39	0.37
Standard deviation (μm)	0.04	0.08	0.15	0.12	0.14	0.15

Refractive index of the $(100-x)MeSiO_{3/2}\cdot xBnSiO_{3/2}$ microparticles increased from 1.40 ($x = 0$) to 1.58 ($x = 100$) with an increase in the content of $BnSiO_{3/2}$, indicating that $MeSiO_{3/2}$ and $BnSiO_{3/2}$

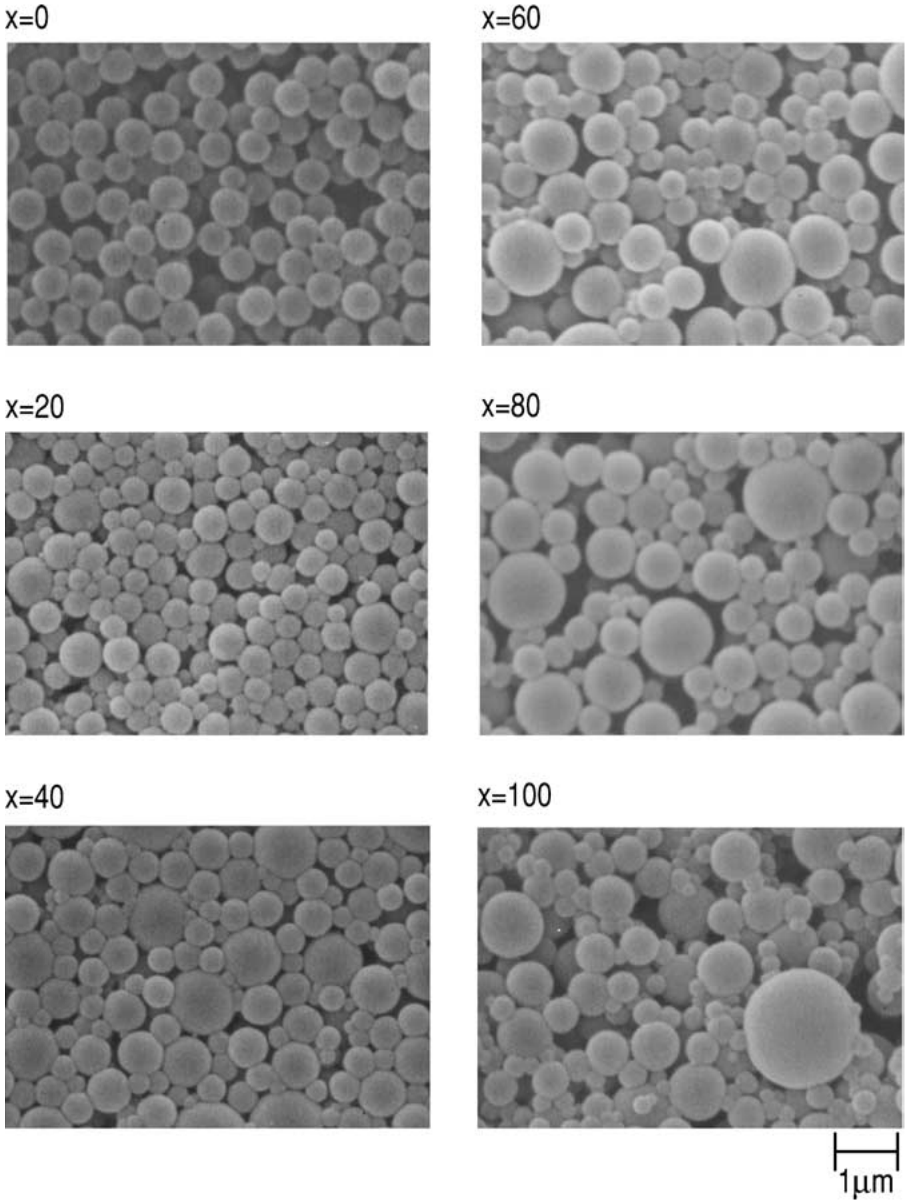

Figure 2 SEM images of the $(100-x)MeSiO_{3/2}\cdot xBnSiO_{3/2}$ ($x = 0$, 20, 40, 60, 80 and 100 mol%) microparticles obtained.

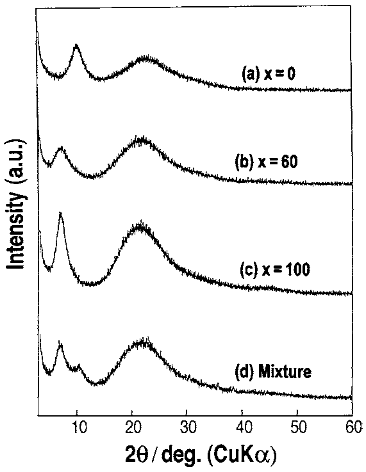

Figure 3 XRD patterns of (a) pure $MeSiO_{3/2}$ microparticles, (b) copolymerized $40MeSiO_{3/2}{\cdot}60BnSiO_{3/2}$ microparticles, (c) pure $BnSiO_{3/2}$ microparticles, and (d) 40:60 (in mol%) mixture of $MeSiO_{3/2}$ microparticles and $BnSiO_{3/2}$ microparticles.

were copolymerized to form organosilsesquioxane particles having both methyl and benzyl groups. Thus, the refractive index of the resultant copolymerized microparticles could be widely controlled by their chemical composition.

Fig. 3 shows XRD patterns of (a) pure $MeSiO_{3/2}$ microparticles, (b) copolymerized $40MeSiO_{3/2}{\cdot}60BnSiO_{3/2}$ microparticles, (c) pure $BnSiO_{3/2}$ microparticles, and (d) 40:60 (in mol%) mixture of pure $MeSiO_{3/2}$ microparticles and pure $BnSiO_{3/2}$ microparticles. All the XRD patterns display a relatively sharp diffraction at around 7–10° and a very broad one at around 21–23°. The sharper diffraction suggests the presence of the structural ordering which is characteristic to silsesquioxanes [16]. The diffraction pattern of (d) 40:60 (in mol%) mixture of $MeSiO_{3/2}$ microparticles and $BnSiO_{3/2}$ microparticles is a convolution of those of (a) pure $MeSiO_{3/2}$ microparticles and (c) pure $BnSiO_{3/2}$ microparticles, whereas the pattern of (b) copolymerized $40MeSiO_{3/2}{\cdot}60BnSiO_{3/2}$ microparticles is different from those of (a) pure $MeSiO_{3/2}$, (c) pure $BnSiO_{3/2}$ and (d) 40:60 mixture. Although ^{29}Si-CPMAS-NMR spectrum of copolymerized $40MeSiO_{3/2}{\cdot}60BnSiO_{3/2}$ microparticles was seemingly composed of the spectra for pure $MeSiO_{3/2}$ and pure $BnSiO_{3/2}$ both of which have two bands assigned to T_2 units with two bridging oxygens and T_3 units with three bridging oxygens, the shape of the spectrum for copolymerized microparticles was different from that of the 40:60 (in mol%) mixture of $MeSiO_{3/2}$ microparticles and $BnSiO_{3/2}$ microparticles. These XRD and NMR results suggest that $MeSiO_{3/2}$ and $BnSiO_{3/2}$ are microscopically hybridized to form microparticles and the nominal composition is achieved for the resultant hybrid particles.

3.2. Thermal sintering properties of microparticles

Two exothermic peaks with weight loss due to burning of organic groups were observed at around 400 and 600°C in DTA-TG curves for copolymerized $40MeSiO_{3/2}{\cdot}60BnSiO_{3/2}$ microparticles. The weight losses at around 400 and 600°C were roughly 30 and 17%, respectively. The disappearance of organic groups such as methyl and benzyl groups after a heat treatment at temperatures higher than 600°C was confirmed from FT-IR spectra. Therefore, the copolymerized $MeSiO_{3/2}$-$BnSiO_{3/2}$ microparticles are thermally stable at temperatures lower than 400°C.

SEM images of $(100 - x)MeSiO_{3/2}{\cdot}xBnSiO_{3/2}$ ($x = 60$, 80 and 100 mol%) microparticles which were stepwise heat-treated at a given temperature for 30 min at 10°C intervals in ambient air are shown in Fig. 4. Fusion between microparticles was observed at 50°C for pure $BnSiO_{3/2}$ (right) and at 70°C for $20MeSiO_{3/2}{\cdot}80BnSiO_{3/2}$ (center), whereas no fusion was observed for the $60MeSiO_{3/2}{\cdot}40BnSiO_{3/2}$ even after a heat treatment at 200°C (left). Thus, the minimum amount of $BnSiO_{3/2}$ to provide the copolymerized $MeSiO_{3/2}$-$BnSiO_{3/2}$ microparticles with thermal sintering properties was estimated to be around 80 mol%.

Fig. 5 shows DSC heating curves from 25 to 70°C for the $(100 - x)MeSiO_{3/2}{\cdot}xBnSiO_{3/2}$ microparticles with $x = 0$, 60, 80 and 100. Neither endo- nor exo-thermic peak is observed in the curve for pure $MeSiO_{3/2}$ ($x = 0$), whereas an endothermic peak due to glass transition is clearly observed at around 40°C for pure $BnSiO_{3/2}$ ($x = 100$). The endo-thermic peaks due to glass transition are also seen in the curves for $40MeSiO_{3/2}{\cdot}60BnSiO_{3/2}$ and

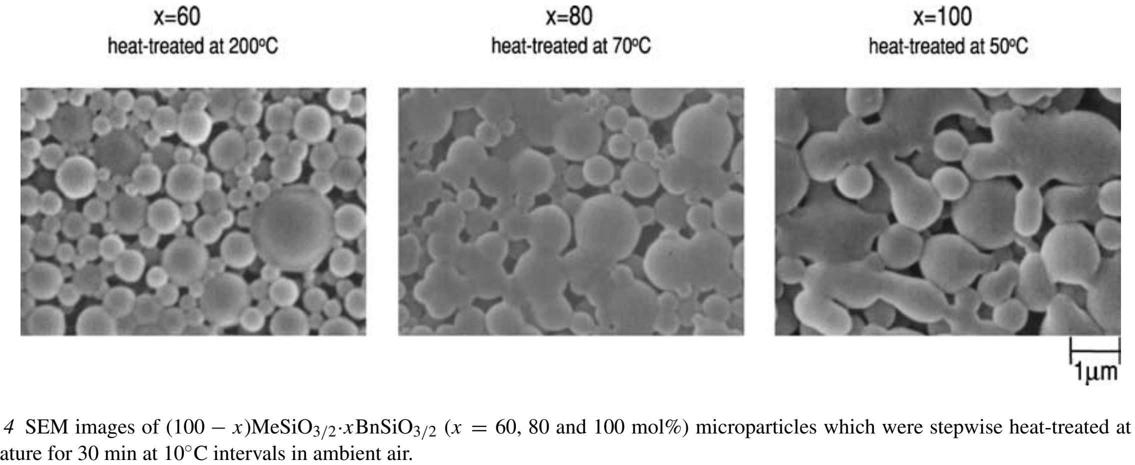

Figure 4 SEM images of $(100 - x)MeSiO_{3/2}{\cdot}xBnSiO_{3/2}$ ($x = 60$, 80 and 100 mol%) microparticles which were stepwise heat-treated at a given temperature for 30 min at 10°C intervals in ambient air.

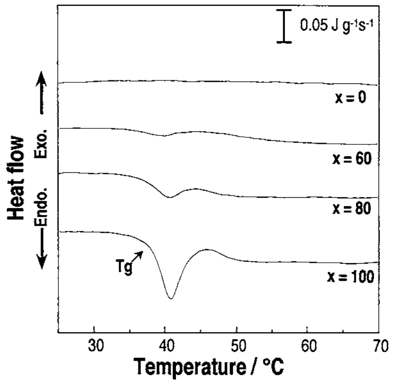

Figure 5 DSC heating curves from 25 to 70°C for the $(100-x)\mathrm{MeSiO}_{3/2}\cdot x\mathrm{BnSiO}_{3/2}$ ($x = 0$, 60, 80 and 100 mol%) microparticles.

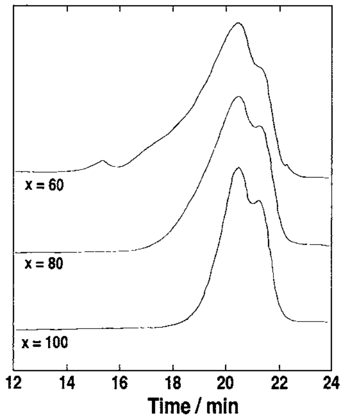

Figure 6 GPC curves of the $(100-x)\mathrm{MeSiO}_{3/2}\cdot x\mathrm{BnSiO}_{3/2}$ ($x = 60$, 80 and 100 mol%) microparticles.

$20\mathrm{MeSiO}_{3/2}\cdot 80\mathrm{BnSiO}_{3/2}$ microparticles, and the peak becomes steeper with an increase in x, i.e., $\mathrm{BnSiO}_{3/2}$ content. These results suggest that the thermal sintering of $\mathrm{MeSiO}_{3/2}$-$\mathrm{BnSiO}_{3/2}$ microparticles is accompanied by a large decrease in viscosity above the glass transition temperature.

Fig. 6 shows GPC curves of the $(100-x)\mathrm{MeSiO}_{3/2}\cdot x\mathrm{BnSiO}_{3/2}$ microparticles with $x = 60$, 80 and 100. In the chromatogram for $40\mathrm{MeSiO}_{3/2}\cdot 60\mathrm{BnSiO}_{3/2}$ microparticles ($x = 60$), a small elusion band is seen at retention time of 15 min, which corresponds to higher molecular weights. When x, i.e., $\mathrm{BnSiO}_{3/2}$ content, in the particles is increased, the elusion band at around 20 min shifts to a longer retention time and the band becomes sharper. These changes in elusion band indicate that the molecular weight itself and molecular weight distribution of $\mathrm{MeSiO}_{3/2}$-$\mathrm{BnSiO}_{3/2}$ microparticles decreased with an increase in $\mathrm{BnSiO}_{3/2}$ content.

3.3. Preparation of thick films by electrophoretic sol-gel deposition

$\mathrm{MeSiO}_{3/2}$-$\mathrm{BnSiO}_{3/2}$ microparticles were negatively charged in the sol and the isostatic point was around pH 4, which is slightly higher than that (ca. pH 2) of pure SiO_2 particles. The $\mathrm{MeSiO}_{3/2}$-$\mathrm{BnSiO}_{3/2}$ microparticles can directly be deposited on ITO-coated glass substrates as an anode by electrophoresis without the collection or redispersion of the particles. The weight of $\mathrm{MeSiO}_{3/2}$-$\mathrm{BnSiO}_{3/2}$ microparticles deposited on the ITO-coated glass substrates increased to be 2 mg cm^{-2} with increasing the applied voltage from 10 to 40 V under a constant deposition time of 3 min. When the applied voltage was higher than 40 V, the films deposited on the edges of the substrates peeled off during the electrophoresis and the resultant films roughened mainly due to the generation of gas from the substrates. The weight of the $\mathrm{MeSiO}_{3/2}$-$\mathrm{BnSiO}_{3/2}$ microparticles also increased to be about 2 mg cm^{-2} with an increase in deposition time from 0 to 15 min under a constant applied voltage of 20 V. The thickness of the as-deposited $(100-x)\mathrm{MeSiO}_{3/2}\cdot x\mathrm{BnSiO}_{3/2}$ microparticles with $x = 60$ and 80 films, for example, reaches to about 4 μm in 10 V for 5 min.

Thick film consisting of electrophoretically deposited pure $\mathrm{BnO}_{3/2}$ microparticles was opaque and became transparent upon thermal sintering of the microparticles during heat treatment at temperatures higher than 100°C. With respect to the electrophoretically deposited thick film of $20\mathrm{MeSiO}_{3/2}\cdot 80\mathrm{BnSiO}_{3/2}$ microparticles, the increase in transmittance in visible range was about 20% after a heat treatment at 200°C for the thermal sintering of the microparticles. The transparency of the $20\mathrm{MeSiO}_{3/2}\cdot 80\mathrm{BnSiO}_{3/2}$ film was not improved even after a heat treatment at 400°C. Elimination of voids and planarization of surface roughness for the deposited film owing to complete thermal sintering should be difficult for the $20\mathrm{MeSiO}_{3/2}\cdot 80\mathrm{BnSiO}_{3/2}$ microparticles, because of the relatively high viscosity of the $20\mathrm{MeSiO}_{3/2}\cdot 80\mathrm{BnSiO}_{3/2}$ upon sintering in comparison with pure $\mathrm{BnO}_{3/2}$. No improvement in transparency was observed for electrophoretically deposited thick film of $40\mathrm{MeSiO}_{3/2}\cdot 60\mathrm{BnSiO}_{3/2}$ microparticles after heat treatments at 200 and 400°C, which can be expected from the no thermal sintering of the microparticles.

Fig. 7 shows typical SEM images of (a) the cross-section of microparticulate $20\mathrm{MeSiO}_{3/2}\cdot 80\mathrm{BnSiO}_{3/2}$ film electrophoretically deposited on ITO-coated glass substrate before heat treatment, (b) the cross-section and (c) the surface of the film after a heat treatment at 200°C for 2 h. The deposition was carried out at 10 V for 5 min. It can be seen from Fig. 7a that as-deposited films consist of the aggregates of the microparticles with diameter of 0.2–0.8 μm. The film shrank from ca. 3.5 to 2.0 μm in thickness after the heat treatment. The surface of the film is still rough even after the heat treatment due to the formation of is let tissue upon thermal sintering of the microparticles as shown in Fig. 7c. This explains the small increase in optical transmittance of the $20\mathrm{MeSiO}_{3/2}\cdot 80\mathrm{BnSiO}_{3/2}$ film during heat treatment and suggests the higher viscosity of $20\mathrm{MeSiO}_{3/2}\cdot 80\mathrm{BnSiO}_{3/2}$ microparticles than that of pure $\mathrm{BnO}_{3/2}$ microparticles upon thermal sintering.

Co-hydrolysis under acidic conditions as well as shortening of co-condensation time under basic conditions in the preparation procedure of the microparticles should be effective ways to reduce the molecular weight of the $\mathrm{MeSiO}_{3/2}$-$\mathrm{BnSiO}_{3/2}$ microparticles and thus to decrease the viscosity of the microparticles upon thermal sintering [14]. The influence of the preparation

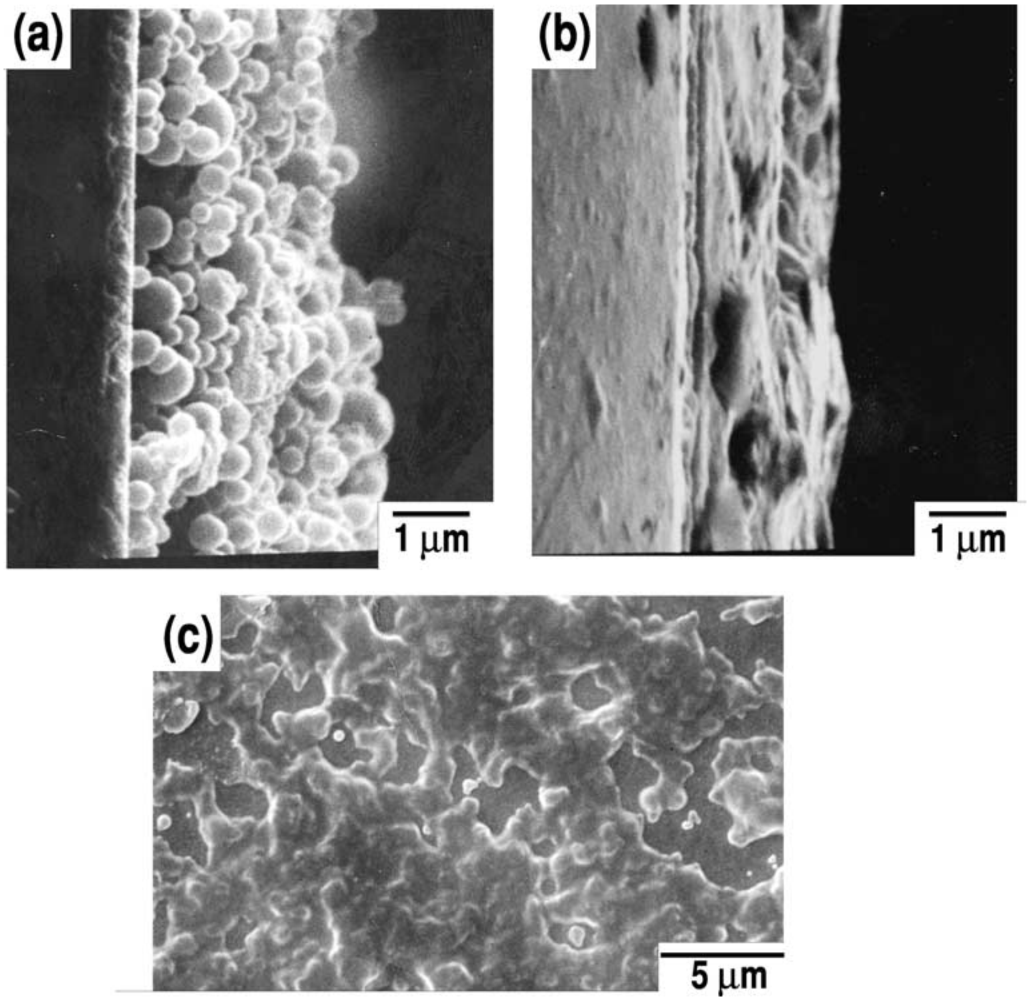

Figure 7 SEM images of (a) the cross-section of microparticulate $20\text{MeSiO}_{3/2}\cdot 80\text{BnSiO}_{3/2}$ film electrophoretically deposited on ITO-coated glass substrate before heat treatment, (b) the cross-section and (c) the surface of the film after a heat treatment at 200°C for 2 h.

conditions of the $\text{MeSiO}_{3/2}$-$\text{BnSiO}_{3/2}$ microparticles on the thermal sintering behavior, and the transparency of the electrophoretically deposited thick films after a subsequent heat treatment are now under study.

4. Conclusion

$\text{MeSiO}_{3/2}$-$\text{BnSiO}_{3/2}$ microparticles obtained were found to be hybrid containing both methyl and benzyl groups. Refractive index of the microparticles increased from 1.42 to 1.58 with an increase in $\text{BnSiO}_{3/2}$ content. The microparticles became fusible at $x \geqq 80$ by a heat treatment at 200°C. Electrophoretically deposited pure $\text{BnO}_{3/2}$ microparticles became highly transparent upon thermal sintering of the microparticles during heat treatment at temperatures higher than 100°C. However, the increase in optical transmittance during the heat treatment of the films consisting of $20\text{MeSiO}_{3/2}\cdot 80\text{BnSiO}_{3/2}$ microparticles was as small as about 20% in visible range even after the heat treatment at 200°C. The smaller increase in transmittance is probably due to the higher viscosity of the $20\text{MeSiO}_{3/2}\cdot 80\text{BnSiO}_{3/2}$ than that of pure $\text{BnO}_{3/2}$ upon thermal sintering for the elimination of voids in the films. Co-hydrolysis under acidic conditions as well as shortening of co-condensation time under basic conditions in the preparation procedure of the microparticles should be effective ways to reduce the molecular weight of the $\text{MeSiO}_{3/2}$-$\text{BnSiO}_{3/2}$ microparticles and thus to decrease the viscosity of the microparticles upon thermal sintering.

Acknowledgments

This work was supported by the Grant-in-Aid from the Ministry of Education, Science, Sports and Culture of Japan.

References

1. S. SAKKA, K. KAMIYA, K. MAKITA and Y. YAMAMOTO, *J. Non-Cryst. Solids* **63** (1984) 223.
2. C. J. BRINKER, A. J. HURD, G. C. FRYE, P. R. SCHUNK and C. S. ASHLEY, *J. Ceram. Soc. Jpn.* **99** (1991) 862.
3. H. KRUNG, N. MERL and H. SCHMIDT, *J. Non-Cryst. Solids* **147/148** (1992) 447.
4. D. R. UHLMANN, S. MOTAKEF, T. SURATWALA, R. WADE, G. TEOWEE and J. M. BOULTON, *J. Sol-Gel Sci. Tech.* **2** (1994) 335.
5. P. SAKAR and P. S. NICHOLSON, *J. Amer. Ceram. Soc.* **79** (1996) 1987.
6. I. ZHITOMIRSKY, *Adv. Coll. Interf. Sci.* **97** (2002) 279.
7. H. NISHIMORI, M. TATSUMISAGO and T. MINAMI, *J. Ceram. Soc. Jpn.* **103** (1995) 78.
8. *Idem.*, *J. Mater. Sci.* **31** (1996) 6529.

9. K. HASEGAWA, S. KUNUGI, M. TATSUMISAGO and T. MINAMI, *Chem. Lett.* (1997) 1115.
10. K. KATAGIRI, K. HASEGAWA, A. MATSUDA, M. TATSUMISAGO and T. MINAMI, *J. Amer. Ceram. Soc.* **81** (1998) 2501.
11. A. MATSUDA, T. SASAKI, K. HASEGAWA, M. TATSUMISAGO and T. MINAMI, *J. Ceram. Soc. Jpn.* **108** (2000) 830.
12. *Idem.*, *J. Amer. Ceram. Soc.* **84** (2001) 775.
13. A. MATSUDA, T. SASAKI, T. TANAKA, M. TATSUMISAGO and T. MINAMI, *J. Sol-Gel Sci. Tech.* **23** (2002) 247.
14. T. SASAKI, A. MATSUDA, T. MINAMI and M. TATSUMISAGO, *J. Ceram. Soc. Jpn.* **101** (2002) 1005.
15. J. Y. CHOI, C. H. KIM and D. K. KIM, *J. Amer. Ceram. Soc.* **81** (1998) 1184.
16. J. F. BROWN, J. F. BROWN, L. H. VOGT, A. KATCHMAN, J. W. EUSTANCE, K. M. KISER and K. W. KRANTZ, *J. Amer. Chem. Soc.* **82** (1960) 6194.

Received 14 February
and accepted 30 June 2003